J Neurosurg 87:307–314, 1997

Microcirculation after cerebral venous occlusions as assessed by laser Doppler scanning

HIROYUKI NAKASE, M.D., OLIVER S. KEMPSKI, M.D., PH.D., AXEL HEIMANN, D.V.M., TOSHIKAZU TAKESHIMA, M.D., AND JAROSLAV TINTERA, PH.D.

Institutes for Neurosurgical Pathophysiology and Neuroradiology, Johannes Gutenberg–University of Mainz, Mainz, Germany

Research on cerebral venous circulation disturbances (CVCDs) has been limited partly by the paucity of animal models that produce consistent venous infarction. Occlusion of two adjacent cortical veins in rats by means of a photochemical thrombotic technique provides a minimally invasive, clinically relevant, and reproducible model suited to study the pathophysiology of CVCDs. In this study, the effects of venous occlusion on regional cortical blood flow and the brain damage that ensues were evaluated.

Cortical vein occlusion was induced by photoactivation of rose bengal via 100-μm fiberoptic illumination. The cerebral venous flow pattern was examined using fluorescence angiography until 90 minutes after venous occlusion, and regional cerebral blood flow (rCBF) was determined at 48 locations by using laser Doppler scanning. Histological damage was assessed 48 hours after vein occlusion. Occlusion of two cortical veins (Group T; seven animals) was compared with single-vein occlusion and its ensuing brain damage (Group S; five animals) and with sham-operated control (five animals). An rCBF reduction occurred 30 minutes after occlusion in Group T and was more extensive than the decrease in Group S after 60 minutes. Observation frequency histograms based on local CBF data obtained in Group T demonstrated that local CBF at some sites decreased to a level below the ischemic threshold within 90 minutes. Six of the seven rats in Group T had a growing venous thrombus with extravasation of fluorescein. The resulting infarction was significantly larger in Group T (9.8 ± 4.5% of the hemispheric area) than in Group S (only 3 ± 1.5% of the hemispheric area).

In conclusion, microcirculation perturbations occur early after venous occlusion and result in the formation of a venous thrombus accompanied by local ischemia and severe venous infarction. The extent of vein occlusion determines the resulting brain damage. Based on the results of this study, the authors conclude that CVCDs may be attenuated by prevention of venous thrombus progression together with the use of protective measures against the consequences of ischemia.

KEY WORDS • cerebral blood flow • cortical vein occlusion • laser Doppler scanning • rat

To date, the consequences of venous occlusion in the brain have been underestimated in neurosurgical practice, and experimental studies of ischemic injury have focused primarily on the effects of arterial occlusion. Recently, however, more attention has been paid to brain injury following perturbations of the cerebral venous circulation because increasing numbers of neurosurgical operations are performed in older-aged patients and because of the development of skull base neurosurgery.[7,8,12,17–19,24,30,32] Therefore, neurosurgical phlebology is gradually maturing as a specialty. Cerebral blood volume (CBV) increases after sinus vein thrombosis (SVT) or cortical vein occlusion. Intracranial hypertension from edema, reductions of regional cerebral blood flow (rCBF), and brain damage can develop secondarily.[4,7–9,27,30,33] More recently, local (l)CBF monitoring has been shown to be useful for predicting brain damage subsequent to SVT or cortical vein occlusion.[19,33] To continue this line of research, further study must be made of the contribution of ischemia mechanisms to the pathophysiological consequences of cerebral venous circulation disturbances (CVCDs). Recently we introduced a potentially useful rat model of photochemically induced venous occlusion that allows selective occlusion of bridging or cortical veins.[18,19] We demonstrated that this nonmechanical method of cortical vein occlusion resulted in a decrease in lCBF, followed by typical pathological changes in the rat brain. Following occlusion of a single vein, this experimental approach is characterized by a high variability in symptoms and histological brain injury in 30% of the animals, whereas, after occlusion of two adjacent veins, brain damage is evident in more than 90% of the animals.[19] Therefore, the occlusion of a single vein is an appropriate model for studies of the variable pathophysiology of venous occlusion observed experimentally as well as in patients, whereas the occlusion of two adjacent veins is a reproducible approach for studies on the pathophysiology and therapy of CVCDs. In the current investigation, patho-

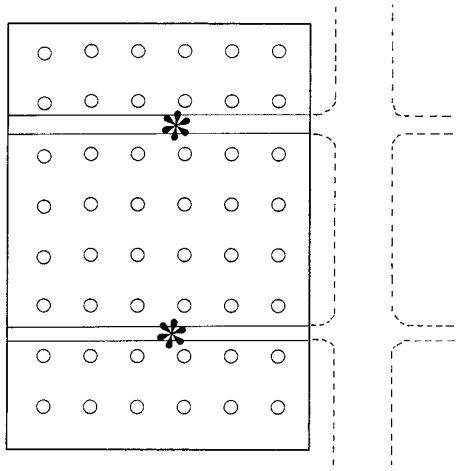

FIG. 1. Illustration of the two–cortical vein occlusion technique and the 48 (8 × 6) grid locations where lCBF was assessed by a scanning procedure using a computer-controlled micromanipulator in the cranial window. The occlusion points are indicated by *asterisks*. In experiments with single-vein occlusion, the 48 locations were similarly arranged with the occlusion site located centrally.

physiological aspects of the cortical microcirculation after CVCDs were studied by means of a laser Doppler (LD) scanning technique[10,14,31,33] in rats with occlusion of two cortical veins. The results were compared with data from single-vein occlusion experiments. The quantitative assessment of brain injury provides the basis for a comparison of experiments with occlusion of one and two cortical veins.

Materials and Methods

This study was conducted in accordance with the German animal protection legislation and has been reviewed by the regional ethics committee (Bezirksregierung Rheinhessen-Pfalz, AZ 177-07/93120).

Animal Preparation

Seventeen male Wistar rats, each weighing between 260 and 340 g, were used for this study: five rats acted as sham-operated controls; seven rats were used for the two-vein occlusion experiments; and data from five rats, which had suffered brain damage after one-vein occlusion in a previous study,[18] were used for comparison. The animals were given free access to food and water in their standard environment prior to surgery. The methods used here have been described in detail previously.[18] Each animal was lightly anesthetized by ether inhalation; anesthesia was maintained by intraperitoneal injection of chloral hydrate (36 mg/100 g wt) after premedication with 0.5 mg atropine. Rectal temperature was kept close to 37°C in all animals. Spontaneous ventilation was maintained throughout the experiment. Polyethylene catheters were placed into the tail artery and the right femoral vein. The arterial catheter was used for continuous monitoring of arterial blood pressure and for blood gas analysis, whereas the venous line was used for administration of fluids and drugs. The PaO_2, $PaCO_2$, and arterial pH were monitored. The head of each animal was placed in a stereotactic frame. Aided by an operating microscope, a 1.5-cm midline skin incision was made and a cranial window (4.5 mm × 6 mm) was created over the right frontoparietal region using a high-speed drill. The drill tip was cooled during the craniotomy by continuous irrigation with physiological saline. The dura mater was left intact and the right frontoparietal cortex was exposed.

Fluorescence Angiography

Fluorescence angiography was performed in all rats. Epicortical vessel structures were studied using a 2% Na^+–fluorescein solution and an excitation source with a wave length of 450 to 490 nm and a No. 12 filter block. A photomacroscope furnished with a 50-W mercury lamp and fluorescence filter was used for fluorescence angiographic studies before and 30 and 90 minutes after induction of venous occlusion. The images were recorded on super-video home system (S-VHS) tape. To minimize damage by fluorescence excitation, illumination was restricted to angiography.

Measurement of CBF Using LD Scanning

Local CBF was registered by a laser flow blood perfusion monitor with a 0.8-mm needle probe and was measured in LD units (LDU). Using a computer-controlled micromanipulator, the probe measured lCBF at 48 locations (in an 8 × 6 grid with 400 μm between location points) with the occluded veins central to the scanning field (Fig. 1). Measurements were taken at 15-minute intervals until 90 minutes after occlusion. Scanning was performed from the beginning to the end of the experiment at identical locations.

Cortical Vein Occlusion by Photochemical Thrombosis

Cortical vein occlusion was induced using rose bengal and fiberoptic illumination (100-μm fiber). Rose bengal was injected slowly, with no effect on arterial pressure, at a dose of 50 mg/kg. Care was taken to avoid illumination of surrounding tissue and other vessels near the target vein(s). The fiber was pointed at a prearranged location on the vein for 10 minutes. In Group T this procedure was repeated for the second vein after an additional injection of a half dose of rose bengal. Complete occlusion of the cortical veins was confirmed later by fluorescence angiography. Thereafter, multiple scanning was repeated every 15 minutes for 90 minutes. After the third fluorescence angiographic study, the resected bone flap was repositioned and the skin wounds were closed. The rats were returned to their individual cages and allowed free access to food and water. The five rats that served as sham-operated controls underwent a craniotomy and rose bengal solution was administered; however, no illumination was made.

Histological Preparation

Two days after the operation the rats were each given an injection of 2% Evans blue dye solution (1 ml/kg) after general anesthesia had been induced with chloral hydrate. After 1 hour, the rats were subjected to perfusion fixation with 4% paraformaldehyde. The brains were removed from the skull and embedded in paraffin to obtain coronal sections of the frontoparietal region. Sections were stained with hematoxylin and eosin.

For quantitative assessment of brain injury, the histological sections were projected onto the screen of a computer using a color charge-coupled device camera and a genlock interface. The optical system was calibrated by using a microscopic ruler. Self-programmed computer software allowed us to measure distances and areas of infarction. The size of the infarction was estimated by evaluating three sections from each brain: the section demonstrating the largest infarction area and sections obtained 0.4 mm anterior and posterior to it. These areas were averaged and expressed as ratios of the ipsilateral and contralateral hemispheric size determined from the respective section.

Magnetic Resonance Imaging

In addition to the experiments already described, three rats from Group T underwent magnetic resonance (MR) imaging 24 hours after surgery. The rats were placed prone on a plastic head holder. A small surface coil (40 mm diameter) was developed in the neuroradiology department to increase the signal-to-noise ratio of MR measurements. The following sequences were used: a T_1-weighted spin-echo sequence with a TR/TE of 400/23 msec (measurement times 6 minutes) and a double spin–echo sequence (proton density and T_2-weighted images) with a $TR/TE_1/TE_2$ of 1800/23/66 msec (measurement time 11 minutes). Measurements were made using a

TABLE 1

*Arterial blood gas levels and MABP sampled before and after venous occlusion in 17 rats**

Group	Before Venous Occlusion (mm Hg)			After Venous Occlusion (mm Hg)		
	PaO_2	$PaCO_2$	MABP	PaO_2	$PaCO_2$	MABP
sham operated (five rats)	81.5 ± 3.4	45.8 ± 5.6	83.2 ± 4.8	80.1 ± 8.0	45.1 ± 3.1	81.4 ± 9.1
Group S (one-vein occlusion; five rats)	83.2 ± 7.7	44.0 ± 2.6	82.3 ± 10.1	86.6 ± 6.5	45.3 ± 3.2	80.3 ± 14.1
Group T (two-vein occlusion; seven rats)	80.1 ± 5.5	45.0 ± 3.0	82.3 ± 7.2	80.7 ± 3.7	44.2 ± 2.6	79.1 ± 5.0

* Values are expressed as means ± SD. There are no statistical differences between any of the groups, or before and after thrombosis induction (analysis of variance, 5% error probability).

2- to 3-mm-slice thickness and a 60-mm field of view (voxel size 0.23 × 0.23 × 3 mm).

Data Management and Statistical Analysis

For mapping of cortical rCBF, lCBF data obtained from 48 locations were plotted according to their topographical origin within the cranial window. Finally a mesh plot was interpolated, in which the z-axis represented lCBF changes (in percentages).

Data are expressed as mean ± standard deviation (SD) for physiological variables and infarction size and as mean ± standard error of the median lCBF found in individual rats. The Mann–Whitney U-test was used to analyze physiological variables such as blood gas levels (PaO_2 and $PaCO_2$), mean arterial blood pressure (MABP), and infarction size. Differences in rCBF were evaluated using analysis of variance (Dunnett's test) for repeated measures and the Kruskal–Wallis test with multiple comparisons between groups. A probability value less than 0.05 was considered statistically significant. Statistical analysis was performed and illustrations were plotted by using commercially available software.

Sources of Supplies and Equipment

Fluorescence angiography was performed using a 2% Na^+–fluorescein solution obtained from E. Merck, Darmstadt, Germany, and a photomacroscope and No. 12 filter obtained from Leitz, Wetzlar, Germany. Images were recorded on HS-S5600E (RS) videotape manufactured by Mitsubishi Electric Corp., Tokyo, Japan. Measurement of lCBF was made using a laser blood flow perfusion monitor (model BPM 403a) purchased from Vasomedics, St. Paul, MN. An Amiga 2000 computer provided by Commodore, Braunschweig, Germany, a color charge-coupled device camera obtained from Sony, Tokyo, Japan, and a Maxigon genlock interface obtained from Merkens EDV, Bad Schwalbach, Germany, were used in the histological study. Calibration of the optic system was made using a microscopic ruler from Leitz. Magnetic resonance imaging was performed using a Gyroscan S15/ACS imaging system obtained from Philips, Hamburg, Germany. To aid data management and statistical analysis, we used Sigma-Plot and Sigma-Stat software purchased from Jandel Scientific, Erkrath, Germany.

Results

Physiological Variables

There were no significant changes in physiological parameters such as blood gas levels (PaO_2 and $PaCO_2$) and MABP during control conditions, after venous occlusion, or among all study groups (Table 1).

Findings on Fluorescence Angiography

Fluorescence angiography provided information about the quality of cerebral venous perfusion and thrombus expansion after vein occlusion. Complete occlusion of the targeted cortical vein and other intact undamaged vessels around the irradiation point were identified using the second fluorescence angiographic study.

No changes were apparent in the sham-operated group, as estimated from three angiographic studies. All vessels, veins in particular, remained well perfused with no evidence of thrombus formation or extravasation of fluorescein. The typical findings on fluorescence angiograms obtained in Group S have been described in detail in a previous communication.[18] Briefly, the second angiographic study showed a flow reversal, a dilation of the distal portion of the occluded vein, and a deceleration of flow. The third angiographic study verified an arrest of flow, further extension of the thrombus, and extravasation of fluorescein into the parenchyma close to the occluded vein. In Group T, similar findings were observed, although the two veins did not necessarily show identical reactions in all cases. Earlier and more extensive extravasation of fluorescence occurred in the parenchyma between the two occluded veins in Group T than around the single occlusion in Group S.

Sequential Changes in rCBF

The calculation of median rCBF values from the 48 locations in each animal demonstrated no change of rCBF during the experiment in the sham-operated group: 54.5 ± 16.5 LDU at the beginning and 62.9 ± 12.4 LDU at the end of the experiment. In Group S, rCBF declined significantly beginning at 1 hour (60, 75, and 90 minutes after occlusion, $p < 0.05$). Regional CBF dropped from 53.8 ± 13.3 LDU during control conditions to 32.5 ± 19.9 LDU at the end of the experiment. On the other hand, rCBF decreased earlier ($p < 0.05$ after 30 minutes) and more dramatically in Group T, as shown in Fig. 2. At 30 minutes, rCBF had decreased from 51.5 ± 10.2 LDU under control conditions to 35 ± 7.3 LDU and continued to decrease to reach 24.4 ± 11 LDU at the end of the experiment. Significant differences were observed between Groups S and T at 30 and 45 minutes after occlusion (Kruskal–Wallis test with multiple comparisons, $p < 0.05$).

Frequency Histograms of lCBF

Frequency histograms of lCBF obtained from LD data demonstrated no change in the sham-operated group during the observation time (data not shown) and a left-shifted distribution 60 minutes after occlusion in Group S. With time this shift to the left became more evident and was most pronounced after 90 minutes, at the end of the experiment (Fig. 3 *left*). Twenty-seven percent of all flow values were below a flow of 20 LDU as compared with only 2.1% during resting conditions. In Group T, the shift to the left occurred earlier (at 30 minutes) and was more

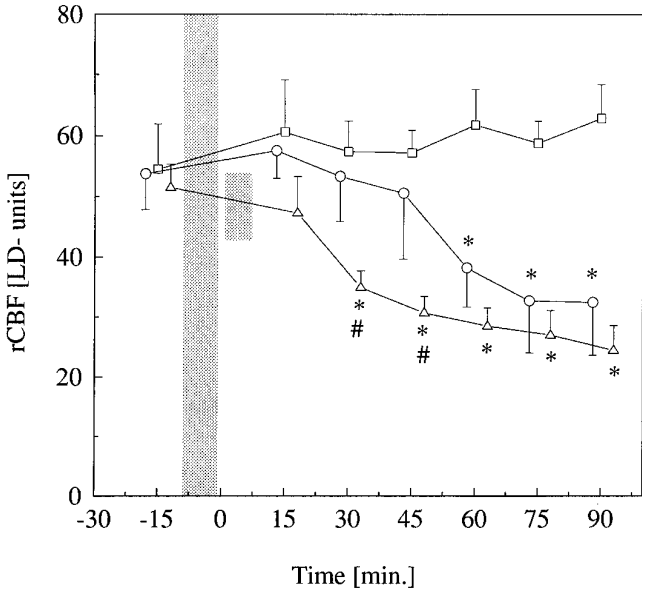

FIG. 2. Graph showing sequential changes in rCBF for each group. The values are expressed in LDU (median ± SEM). *Gray bars* indicate the illumination of the veins. In the single-vein occlusion group (Group S; *circles*), rCBF significantly decreased (60, 75, and 90 minutes postocclusion, *$p < 0.05$). In the two-vein occlusion group (Group T: *triangles*), rCBF was significantly reduced beginning 30 minutes after occlusion. Significant differences between Group S and Group T are indicated. (#$p < 0.05$). Sham-operated control animals are indicated by *squares*.

pronounced, with 39.6% of all cortical locations showing flow values below 20 LDU after 90 minutes, that is, in a possibly ischemic range found under control conditions in only 6% of all cases in this group (Fig. 3 *right*).

Cortical CBF Mapping

Cortical CBF mapping demonstrated a transient hyperperfusion zone around a hypoperfused ischemic core in three of the five animals in Group S and a hypoperfused ischemic area around two occluded veins in six of the seven animals from Group T in the early stage. A massive and widespread decrease in lCBF in the cranial window was seen in both groups in the later stage (Fig. 4).

Magnetic Resonance Imaging

The coronal view of the T_1-weighted images showed a low-intensity lesion (not shown), and the T_2-weighted images revealed a high-intensity area of biconvex shape centering around the occluded veins in all three Group T rats tested (Fig. 5).

Histological Studies

Histopathological observations confirmed that the brains of the sham-operated animals appeared normal. In Group S, all five rats had parenchymal damage, such as multiple petechial hemorrhages surrounding the dilated capillaries (one rat) and edematous areas in the white and gray matter with extravasation of Evans blue dye and tissue damage (all rats). Six of the seven rats in Group T showed more extensive petechial hemorrhage and infarction. Quantitative assessment of brain injury (Fig. 6), which was expressed as a percentage of the ipsilateral hemisphere, showed a significantly larger infarction size in Group T (9.8 ± 4.5 %) than in Group S (3 ± 1.5%) (Mann–Whitney U-test, $p < 0.05$). When expressed as a ratio of the contralateral hemisphere, brain injury was again significantly ($p < 0.05$) greater in Group T (10.9 ± 5.5%) than in Group S (3.1 ± 1.6%).

Discussion

Rat Cortical Vein Occlusion Using the Photochemical Thrombotic Technique

Until recently, very little was known about the pathophysiology of CVCDs. The paucity of suitable animal models has, in part, impaired the development of research on CVCDs, and technical difficulties have precluded studies of the selective occlusion of bridging and cortical veins thus far. We introduced a rat model of cortical vein occlusion involving the use of the photochemical thrombotic technique, which has little local or systemic side effects, is easy to perform, and is clinically relevant. Moreover, the rat model clearly has some advantages over large-animal models.[19] It is also a model for the intraoperative sacrifice of cortical veins during neurosurgical operations. The photothrombotic occlusion technique was originally established to perform arterial occlusions.[20,35]

The underlying mechanism is aggregation of platelets at the endothelial luminal surface after photochemical induction of local singlet oxygen production. Platelet–endothelial cell and platelet–platelet interactions are integral to the model. Nakayama, et al.,[20] who occluded the rat middle cerebral artery by using this technique and recanalized it by topical application of the calcium entry blocker nimodipine demonstrated that the resulting endothelial damage consisted only of a mild luminal discontinuity and surface projections. In addition, we could not detect any cell damage after exposure of cultured endothelial cells to rose bengal and light (data not shown). Furthermore, we have already verified the absence of any influence on cerebral parameters (for instance, CBF, CBV fraction, and histological structures) and global physiological parameters (such as systemic blood pressure, heart rate, arterial pH, PaO_2, $PaCO_2$, and hematocrit) by means of either irradiated controls without dye injection or controls with dye injection and no illumination.[18,19] However, after rose bengal application, the brain is temporarily sensitive to light wavelengths of 500 to 600 nm, and much care should be taken to avoid illumination of tissues and other vessels next to the target vein.

The occlusion of two adjacent veins (Group T) is a reliable model for studying CVCDs. Compared with the solitary vein occlusion model (Group S), rCBF decreased earlier and more severely in the two-vein occlusion model and infarction size was larger, that is, the extent of CBF reduction reflected the subsequent parenchymal damage. Only a fraction of animals with solitary vein occlusion (summarized here in Group S) developed infarction,[18] whereas most rats with dual vein occlusion suffered parenchymal damage. In this group, individual cortical locations already showed critically low flow values during the

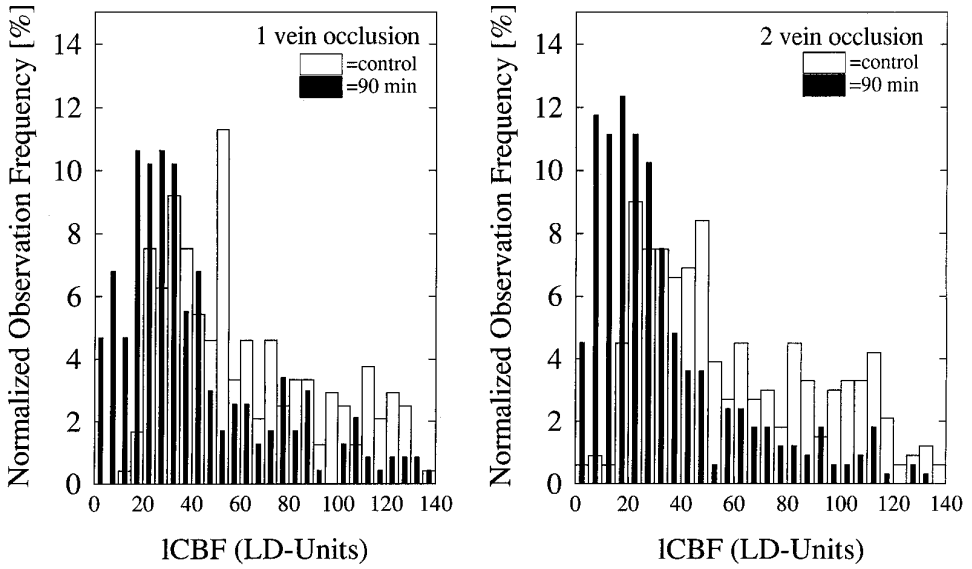

FIG. 3. Observation frequency histograms of lCBF obtained by LD scanning in all rats in Group S *(left)* and Group T *(right)* during control conditions *(open bars)* and 90 minutes after occlusion *(filled bars)*. Histograms are obtained by assigning measurements to flow classes and counting observation frequencies for each class. In this study, 240 measurements (five rats, 48 locations) were used to calculate the histogram for Group S, and 336 for Group T (seven rats, 48 locations). The typical lCBF pattern before vein occlusion is characterized by a left-shifted distribution with a frequency maximum between 20 and 50 LDU. Note that less than 6% of observations in the flow classes were below 20 LDU during control conditions. A median of 90 minutes after occlusion, a dramatic shift in distribution to the left occurred and flow values below 20 LDU increased. Low flow measurements were more frequently observed in Group T.

experiment. These results demonstrate that occlusion of more than one vein gives rise to earlier and more extensive lCBF decreases, resulting in more severe brain damage than solitary vein occlusion.

Laser Doppler Scanning Technique

Laser Doppler flowmetry, which enables tissue perfusion to be recorded noninvasively and continuously,[5,28] is no longer considered only a research tool but is also used in clinical investigations.[13,23] In the LD scanning technique proposed here, the LD probe is directed by a computer-controlled motorized micromanipulator to multiple predefined positions in the cranial window to measure lCBF at many different sites. The data are used to calculate typical rCBF observation frequency histograms and for cortical CBF mapping. Based on the variability of CBF results ob-

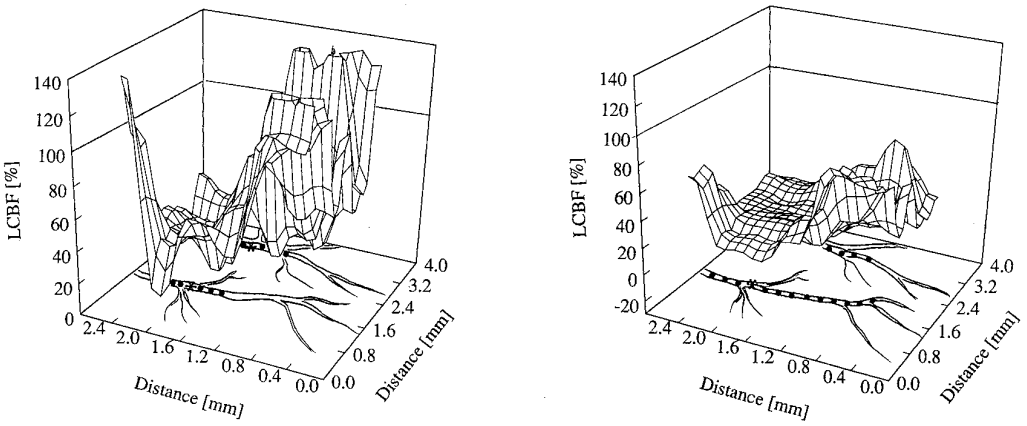

FIG. 4. *Left:* Cortical lCBF mapping 30 minutes after induction of thrombus in a typical experiment using a Group T rat. Data are expressed in percentage change from the individual baseline value determined for each location. The anatomy of the occluded vein and the location of the thrombus are indicated. The growing thrombus is indicated by *black dots*. The mapping reveals a hypoperfusion area in the parenchyma between occluded vein in the very early period, that is, 30 minutes after occlusion. *Right:* Cortical lCBF mapping 90 minutes after vein occlusion in the same animal shown *left*. The thrombus has grown and the mapping reveals an extensive decrease in rCBF.

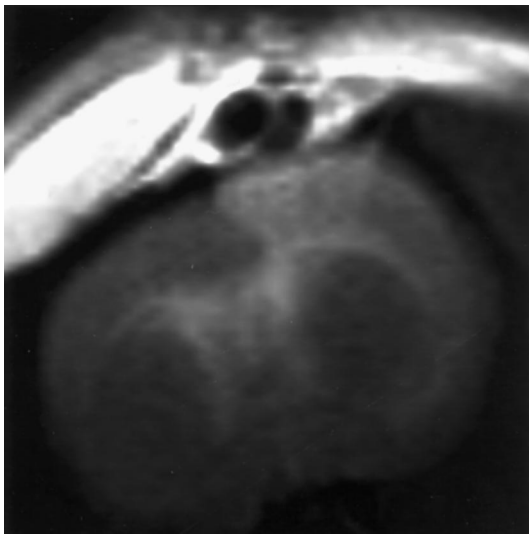

FIG. 5. Magnetic resonance T_2-weighted image obtained 24 hours after two–cortical vein occlusion. Coronal view of the head shows high-intensity area of biconvex shape around the occluded veins.

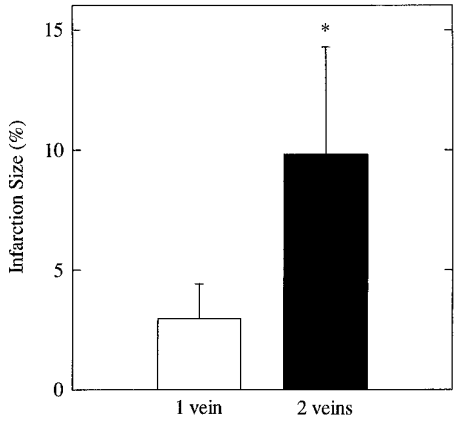

FIG. 6. Bar graph depicting quantitative assessment of infarction size, expressed as a percentage of the size of the ipsilateral hemisphere, in Group S (one vein) and Group T (two veins). Infarction size was significantly larger in Group T than in Group S (*$p < 0.05$).

tained in this procedure, compared with those found with other techniques,[1,16,26] information gathered from a sufficient number of locations can compensate, in part, for the inability of the LD technique to express CBF in absolute terms.[17] Cortical CBF mapping provides information on lCBF in individual locations. We reported that the mapping showed a transient hyperperfusion area adjacent to the ischemic area surrounding an occluded vein in Group S.[18] This hyperperfusion zone, which may be equivalent to luxury perfusion[15] or border-zone hyperemia[21] in arterial occlusion, was found at a very early stage following venous occlusion and changed to a hypoperfusion zone thereafter. In the present study we observed CBF reduction in the area between the two occluded veins, whereas hyperperfusion around this ischemic area might have occurred outside the cranial window, although not documented in the present experimental setting.

Pathophysiology During CVCDs

The exact pathophysiological mechanisms underlying the high variety of symptoms observed in patients and experimental animals following CVCDs are still unclear, although our data indicate that individual availability of collateral vessels determines outcome. Previous investigations in this laboratory revealed that 71% (12 of 17) of animals tolerated occlusion of a solitary vein without major flow disturbances or brain damage.[18] The rats used in Group S were the five remaining animals. In the present study we have demonstrated that growing venous thrombus accompanied by critically low local cortical flow values occurred at a much earlier stage in animals with brain injury after CVCDs than was generally expected. Although histological assessment was performed 48 hours after occlusion, MR imaging could already detect the cerebral venous infarction 24 hours earlier. Magnetic resonance imaging is a promising diagnostic tool that can replace angiography for the diagnosis of dural sinus thrombosis.[11,22] The signal characteristics of a thrombus and lack of flow in the sinus on MR imaging are well known, and recently the patterns of parenchymal and vascular changes on MR imaging have been documented.[36]

Increased CBV, vasogenic edema due to venous congestion with secondary cerebral ischemia, and subsequent cytotoxic edema have been considered to be the main pathophysiological mechanisms after CVCDs in the brain.[7,9] We have already reported a temporary increase in CBV before the decrease in CBF in Group S.[18] Valtysson and colleagues[34] showed that a brief, sudden, and transient elevation in intracranial pressure increases the size of infarction after middle cerebral artery occlusion in the rat. In CVCDs, increased CBV and decreased CBF might produce a cumulative detrimental effect on the brain. Sakaki, et al.,[25] reported that drastic and continuing retraction is more deleterious than cerebral vein occlusion, and the combination of these two factors has a much more harmful effect, which leads to extensive venous infarction in the cat brain.

Kanno and associates[12] examined lCBF before and after temporary clipping of cortical veins and sinus and recommended preservation of the venous system if CBF decreases significantly after temporary occlusion, especially if the decrease is above 10 ml/minute/100 g.

Therapy for CVCDs

Fries and coworkers[8] described a multistep evolution of pig SVT and proposed that the best way to prevent progression of SVT into the cortical veins is to interfere with the growth of the thrombus by anticoagulation. Frerichs, et al.,[7] also demonstrated a beneficial effect of heparin, as shown by the reversal of the pathological impedance increase, which could be interpreted as a reduction in cytotoxic edema. It might be advisable to use heparin,[6] thrombolysis,[3,29] and venous revascularization,[24] if applicable, as long as venous flow and CBF are preserved.

As a primary conclusion on the basis of the current data, therapy of CVCDs should include preventive measures to interrupt the growth of the venous thrombus. In particular,

those tissues that exhibit a low flow zone in the vicinity of thrombosed veins have a potential to recover and resemble tissues in the ischemic penumbra[2] surrounding an arterial infarct.[17,18] The model used in our experiments is a good approximation of the intraoperative sacrifice of cortical veins. Therefore, the current study is of clinical interest, especially for the prediction of brain injury following CVCDs by intraoperative CBF monitoring (for example, LD flowmetry measurement, thermal diffusion measurements, and transcranial Doppler blood velocity monitoring), postoperative CBF studies (such as single-photon emission computerized tomography and stable xenon–computerized tomography scanning), or neuroradiological examination (MR imaging and angiography). In the future it might also have an impact on therapeutic considerations: CVCDs should be treated fast and vigorously, with a primary focus on attempts to increase lCBF and inhibit thrombosis progression, in combination with using antiischemic agents such as glutamate antagonists or free radical scavengers. This study can at least provide experimental evidence for the treatment of CVCDs. However, the present results cannot be directly translated to proposed treatment regimens in human cerebral vein thrombosis. Clearly, further studies for the treatment of human disease are needed.

Conclusions

One of the pathophysiological consequences of CVCDs is certainly hypoperfusion of circumscribed brain areas drained by the occluded veins. In some of these territories the supply of blood may fall below a critical threshold, resulting in an ischemic or hypoxemic lesion. The comparison of a model of solitary vein occlusion with one of dual vein occlusion has shown that the extent of vein occlusion determines the size of parenchymal injury. Moreover, inhibition of the growth of the thrombus together with antiischemic measures could impede the development of CVCDs. The use of the photochemical dye technique to produce cerebral venous occlusion is a worthwhile addition to study circulation perturbations of the brain.

Acknowledgments

The authors wish to express their gratitude to Monika Westenhuber for excellent secretarial assistance and to Michael Malzahn, Laszlo Kopacz, and Andrea Schollmayer for technical help and support.

References

1. Anderson RE, Meyer FB, Tomlinson FH: Focal cortical distribution of blood flow and brain pH_i determined by *in vivo* fluorescent imaging. **Am J Physiol 263:**H565–H575, 1992
2. Astrup J, Siesjö BK, Symon L: Thresholds in cerebral ischemia—the ischemic penumbra. **Stroke 12:**723–725, 1981
3. Barnwell SL, Higashida RT, Halbach VV, et al: Direct endovascular thrombolytic therapy for dural sinus thrombosis. **Neurosurgery 28:**135–142, 1991
4. Cervos-Navarro J, Kannuki S: Neuropathological findings in the thrombosis of cerebral veins and sinuses: vascular aspects, in Einhäupl K, Kempski O, Baethmann A (eds): **Cerebral Sinus Thrombosis. Experimental and Clinical Aspects.** New York: Plenum, 1990, pp 15–25
5. Dirnagl U, Kaplan B, Jacewicz M, et al: Continuous measurement of cerebral blood flow by laser-Doppler flowmetry in a rat stroke model. **J Cereb Blood Flow Metab 9:**589–596, 1989
6. Einhäupl KM, Villringer A, Meister W, et al: Heparin treatment in sinus venous thrombosis. **Lancet 338:**597–600, 1991
7. Frerichs KU, Deckert M, Kempski O, et al: Cerebral sinus and venous thrombosis in rats induces long-term deficits in brain function and morphology—evidence for a cytotoxic genesis. **J Cereb Blood Flow Metab 14:**289–300, 1994
8. Fries G, Wallenfang T, Hennen J, et al: Occlusion of the pig superior sagittal sinus, bridging and cortical veins: multistep evolution of sinus-vein thrombosis. **J Neurosurg 77:**127–133, 1992
9. Gotoh M, Ohmoto T, Kuyama H: Experimental study of venous circulatory disturbance by dural sinus occlusion. **Acta Neurochir 124:**120–126, 1993
10. Heimann A, Kroppenstedt S, Ulrich P, et al: Cerebral blood flow autoregulation during hypobaric hypotension assessed by laser Doppler scanning. **J Cereb Blood Flow Metab 14:** 1100–1105, 1994
11. Isensee C, Reul J, Thron A: Magnetic resonance imaging of thrombosed dural sinuses. **Stroke 25:**29–34, 1994
12. Kanno T, Kasama A, Shoda M, et al: [Intraoperative monitoring on the occlusion of the venous system.] **Neurosurgeons 11:** 51–59, 1992 (Jpn)
13. Kawaguchi T, Fujita S, Hosoda K, et al: [Multi-modality and multi-channel monitoring system during aneurysmal surgery.] **Surg Cereb Stroke 22:**373–378, 1994 (Jpn)
14. Kempski O, Heimann A, Strecker U: On the number of measurements necessary to assess regional cerebral blood flow by local laser Doppler recordings: a simulation study with data from 45 rabbits. **Int J Microcirc Clin Exp 15:**37–42, 1995
15. Lassen NA: The luxury-perfusion syndrome and its possible relation to acute metabolic acidosis localised within the brain. **Lancet 2:**1113–1115, 1966
16. Nakai H, Yamamoto YL, Diksic M, et al: Triple-tracer autoradiography demonstrates effects of hyperglycemia on cerebral blood flow, pH, and glucose utilization in cerebral ischemia of rats. **Stroke 19:**764–772, 1988
17. Nakase H, Heimann A, Kempski O: Alterations of regional cerebral blood flow and tissue oxygen saturation in a rat sinus-vein thrombosis model. **Stroke 27:**720–728, 1996
18. Nakase H, Heimann A, Kempski O: Local cerebral blood flow in a rat cortical vein occlusion model. **J Cereb Blood Flow Metab 16:**720–728, 1996
19. Nakase H, Kakizaki T, Miyamoto K, et al: Use of local cerebral blood flow monitoring to predict brain damage after disturbance to the venous circulation: cortical vein occlusion model by photochemical dye. **Neurosurgery 37:**280–286, 1995
20. Nakayama H, Dietrich WD, Watson BD, et al: Photothrombotic occlusion of rat middle cerebral artery: histopathological and hemodynamic sequelae of acute recanalization. **J Cereb Blood Flow Metab 8:**357–366, 1988
21. Olsen TS, Larsen B, Skriver EB, et al: Focal cerebral hyperemia in acute stroke. Incidence, pathophysiology and clinical significance. **Stroke 12:**598–607, 1981
22. Padayachee TS, Bingham JB, Graves MJ, et al: Dural sinus thrombosis. Diagnosis and follow-up by magnetic resonance angiography and imaging. **Neuroradiology 33:**165–167, 1991
23. Rosenblum BR, Bonner RF, Oldfield EH: Intraoperative measurement of cortical blood flow adjacent to cerebral AVM using laser Doppler velocimetry. **J Neurosurg 66:**396–399, 1987
24. Sakaki T, Hoshida T, Morimoto T, et al: [Cerebral venous disturbance and surgical treatment.] **Neurosurgeons 11:**96–105, 1992 (Jpn)
25. Sakaki T, Kakizaki T, Takeshima T, et al: Importance of prevention from intravenous thrombosis and preservation of the venous collateral flow in bridging vein injury during surgery: an experimental study. **Surg Neurol 44:**158–162, 1995

26. Sako K, Kobatake K, Yamamoto YL, et al: Correlation of local cerebral blood flow, glucose utilization, and tissue pH following a middle cerebral artery occlusion in the rat. **Stroke 16:** 828–834, 1985
27. Sato S, Toya S, Ohtani M, et al: The effect of sagittal sinus occlusion on blood-brain barrier permeability and cerebral blood flow in the dog, in Inaba Y, Klatzo I, Spatz M (eds): **Brain Edema.** Berlin: Springer-Verlag, 1985, pp 235–239
28. Skarphedinsson JO, Hårding H, Thorén P: Repeated measurements of cerebral blood flow in rats. Comparisons between the hydrogen clearance method and laser Doppler flowmetry. **Acta Physiol Scand 134:**133–142, 1988
29. Smith TP, Higashida RT, Barnwell SL, et al: Treatment of dural sinus thrombosis by urokinase infusion. **AJNR 15:**801–807, 1994
30. Takeshima T, Miyamoto K, Okumura Y, et al: Experimental study of local cerebral blood flow in cerebral venous occlusion, in Tomita M, Mchedlishvili G, Rosenblum BR, et al (eds): **Microcirculatory Stasis in the Brain.** Amsterdam: Elsevier, 1993, pp 441–450
31. Ulrich P, Kroppenstedt S, Marchand C, et al: Reserve capacity tested by acetazolamide response of cortical microflow up to six weeks after permanent bilateral occlusion of the common carotid artery in rats. **J Cereb Blood Flow Metab 13 (Suppl 1):**S210, 1993 (Abstract)
32. Ungersböck K, Heimann A, Kempski O: Cerebral blood flow alterations in a rat model of cerebral sinus thrombosis. **Stroke 24:**563–570, 1993
33. Ungersböck K, Heimann A, Strecker U, et al: Mapping of cerebral blood flow by laser-Doppler flowmetry, in Tomita M, Mchedlishvili G, Rosenblum, et al (eds): **Microcirculatory Stasis in the Brain.** Amsterdam: Elsevier, 1993, pp 405–413
34. Valtysson J, Jiang M, Persson L: Transient elevation of the intracranial pressure increases the infarct size and perifocal edema after subsequent middle cerebral artery occlusion in the rat. **Neurosurgery 30:**887–890, 1992
35. Watson BD, Dietrich WD, Prado R, et al: Argon laser-induced arterial photothrombosis. Characterization and possible application of therapy of arteriovenous malformations. **J Neurosurg 66:**748–754, 1987
36. Yuh WTC, Simonson TM, Wang AM, et al: Venous sinus occlusive disease: MR findings. **AJNR 15:**309–316, 1994

Manuscript received November 14, 1996.
Accepted in final form February 6, 1997.
Address reprint requests to: Oliver Kempski, M.D., Ph.D., Institute for Neurosurgical Pathophysiology, Johannes Gutenberg–University of Mainz, Langenbeckstrasse 1, 55101 Mainz, Germany.